Atmos. Meas. Tech., 19, 2881–2895, 2026
https://doi.org/10.5194/amt-19-2881-2026

Atmospheric Measurement Techniques
Open Access
EGU

Exploring the potential of aerial and balloon-based observations in the study of terrestrial gamma ray flashes

Marek Sommer[1], **Tomáš Czakoj**[2], **Iva Ambrožová**[1], **Martin Kákona**[1,3], **Olena Velychko**[1,4], **and Ondřej Ploc**[1]

[1]Department of Radiation Dosimetry, Nuclear Physics Institute of the Czech Academy of Sciences, Husinec – Řež 130, 250 68 Řež, Czech Republic
[2]Neutron Physics Department, Centrum Výzkumu Řež s.r.o., Husinec – Řež 130, 250 68, Czech Republic
[3]Department of Space Physics, Institute of Experimental Physics of the Slovak Academy of Sciences, Watsonova 47, Košice 040 01, Slovak Republic
[4]Faculty of Nuclear Sciences and Physical Engineering, Czech Technical University in Prague, Břehová 7, 115 19 Prague, Czech Republic

Correspondence: Marek Sommer (sommer@ujf.cas.cz)

Received: 6 September 2024 – Discussion started: 14 October 2024
Revised: 1 June 2025 – Accepted: 12 June 2025 – Published: 29 April 2026

Abstract. Recently presented measurements of terrestrial gamma ray flashes (TGFs) above thunderstorms on board aircraft and weather balloons introduce viable alternatives which could help to overcome limitations inherent in satellite-based observations, such as gamma ray attenuation by the atmosphere and large distance between TGF source and detectors. This study explores the potential and implications of measuring TGFs using aircraft and weather balloons. Utilizing Monte Carlo simulations with the MCNP6 tool, the spatial distributions, fluences, and energy spectra of photons, electrons, and neutrons generated by TGFs are assessed at altitudes of 5 to 50 km. The results indicate that TGFs originating at lower altitudes produce narrower beams compared to those at higher altitudes, suggesting that weather balloons may be more effective for high-altitude TGFs, such as those associated with summer thunderstorms or thunderstorms in tropical regions, whereas staffed aircraft might be more suitable for low-altitude TGFs originating in temperate regions or in winter thunderstorms. Features of the photon and electron energy spectra, such as maximum energy and the presence of 511 keV photons, can help estimate the radial distance from the TGF axis. Expected photon fluences from TGFs reach up to 1000 cm^{-2}, with electron fluences reaching up to 100 cm^{-2}, depending on the TGF's brightness. Neutron fluences are notably lower, up to 1 cm^{-2}. These findings underscore the potential of aerial and balloon-based measurements in providing critical insights into TGFs and their detection, addressing the limitations of current satellite observations.

1 Introduction

The phenomenon of terrestrial gamma ray flashes (TGFs) was discovered in 1994 by Fishman et al. (1994). TGFs are associated with lightning, during which extremely intense bursts of radiation are emitted within hundreds of microseconds (Cummer et al., 2011, 2015; Østgaard et al., 2021; Marisaldi et al., 2019). Thousands of TGFs have been observed and registered on board the International Space Station (ISS), satellites, airplanes (Smith et al., 2011; Bowers et al., 2018; Bjørge-Engeland et al., 2024; Ostgaard et al., 2024a), and weather balloons (Helmerich et al., 2024), as well as and on the ground (so-called downward TGFs) (Dwyer et al., 2004; Tran et al., 2015; Hare et al., 2016; Enoto et al., 2017; Wada et al., 2019; Belz et al., 2020). The majority of TGFs have been detected by detectors on satellites, namely the Reuven Ramaty High Energy Solar Spectroscopic Imager (RHESSI) (Smith et al., 2005; Grefenstette et al., 2009), the Astrorivelatore Gamma a Immagini Leggero (AGILE) (Marisaldi et al., 2010, 2014; Maiorana et al., 2020), the Gamma-ray Burst Monitor (GBM) on board the Fermi Gamma-ray Space Telescope (Briggs et al., 2010, 2013; Roberts et al., 2018), and the Atmosphere–

Space Interactions Monitor (ASIM) on board the International Space Station (Østgaard et al., 2019; Neubert et al., 2019).

Most of the detected TGFs were registered at low latitudes, mainly due to the low inclination of the satellites. However, it has been observed that there is a lower TGF-to-lightning ratio in latitudes over 30°. Maiorana et al. (2021) proposed that this dependence is mainly caused by atmospheric absorption of gamma rays due to the elevated tropopause in equatorial regions.

The number of bremsstrahlung photons generated during TGFs has been a topic of extensive discussion, with estimates ranging from 10^{17} to 10^{20} gamma rays (Dwyer and Smith, 2005; Gjesteland et al., 2015). More recently, the existence of TGFs with significantly lower intensities, ranging from 10^{12} to 10^{15} gamma rays, was confirmed by Bjørge-Engeland et al. (2024). This discovery suggests that satellite-based measurements capture only a fraction of all TGFs. The possibility of such lower-intensity TGFs was theorized in Østgaard et al. (2012), while Celestin et al. (2015) proposed a mechanism to explain their generation. The energy spectrum of gamma rays reaches very high energies, up to tens of megaelectronvolts (Grefenstette et al., 2009; Marisaldi et al., 2010; Tavani et al., 2011; Marisaldi et al., 2019).

Despite numerous observations and studies of various TGFs, the mechanisms of their origin, particularly those responsible for generating such a large number of energetic photons in the megaelectronvolt range, are not yet fully understood. A widely accepted foundation involves runaway electrons producing bremsstrahlung radiation through the relativistic runaway electron avalanche (RREA) process. Building upon this, several theories continue to be investigated (Dwyer, 2008; Celestin and Pasko, 2011; Petrov, 2021; Zelenyi et al., 2019; Stadnichuk et al., 2021, 2023), exploring different aspects and extensions of this fundamental mechanism. Among these, two primary mechanisms based on RREA have been proposed, differing in their predicted beaming geometries. In the first mechanism, a RREA develops within a large-scale electric field (Dwyer, 2003), accelerating electrons predominantly in a vertical direction, resulting in a narrow photon beam concentrated within a small cone. In contrast, the second mechanism assumes electron acceleration in the lightning leader tip, where the geometry of the electric field leads to a broader angular distribution of electrons (Celestin and Pasko, 2011), producing a wider photon emission cone (30–40°).

The beaming geometry of satellite-based TGF measurements was investigated in Hazelton et al. (2009), Gjesteland et al. (2011), Mailyan et al. (2016), Mailyan et al. (2019), and Lindanger et al. (2021). In Mailyan et al. (2016) and Mailyan et al. (2019), the authors included the propagation of accelerated electrons in their simulations. To obtain a wide geometry, they artificially introduced a wide cone distribution of bremsstrahlung photons with a certain half angle. Narrow beaming was modeled by introducing no changes in the bremsstrahlung angular distribution. In contrast, Hansen et al. (2013), Marisaldi et al. (2019), and Lindanger et al. (2021), Ursi et al. (2022) skipped the simulation of electrons and modeled only the propagation of bremsstrahlung photons, assuming an initial cone with various half angles. Such an approach has a limitation. The beaming geometry of TGFs depends on altitude due to variations in air density and composition, which affect both bremsstrahlung emission and electron and photon interactions with air molecules. The studies of Mailyan et al. (2016) and Mailyan et al. (2019), which accounted for electron propagation, showed that the distinction between narrow and wide beaming is not straightforward as they found that out of 66 analyzed TGFs, 24 were best fitted by narrow models, and 15 were best fitted by wide RREA models, while Hazelton et al. (2009) and Lindanger et al. (2021) concluded that a wide beaming geometry is preferred. Hazelton et al. (2009) used cumulative TGF energy spectra, whereas Mailyan et al. (2016), Mailyan et al. (2019), and Lindanger et al. (2021) analyzed the energy spectra of individual TGFs. Moreover, the results of analysis in Bjørge-Engeland et al. (2024) indicate that TGFs detected on board the ER-2 aircraft had a wide geometry with a half angle of 30°.

In our study, we considered only narrow-beaming scenarios for simplicity. However, we acknowledge that this is a significant limitation, as it does not account for the possibility of wider beaming geometries that could arise under different physical conditions. This simplification must be kept in mind when interpreting our results.

While most studies focus on satellite-based detections, an increasing number of TGFs have been observed from the ground and airborne platforms in recent years. Nevertheless, the majority of TGF detections still come from space-based instruments. Measurements from Earth's orbit have several disadvantages, such as a low number of registered photons due to the large distance between the source and detector; blurring of the TGF time structure – primarily at low energies – due to Compton scattering; and the high speed of the satellite, which prevents them from staying above a thunderstorm for a long period of time. These factors complicate the study of TGF energy spectra and time structure and observations of TGFs at mid-latitudes.

As recognized by Lyu et al. (2023), significant new discoveries may arise from joint measurements of a single event from both below and above, involving on-ground and orbital observations. Due to their high velocities, satellites are limited in their ability to focus on a single thunderstorm over an extended period. However, airplanes and weather balloons offer a viable alternative, as they can be strategically positioned in or above thunderstorms to monitor TGF activity, potentially yielding insights that satellites cannot. A recent study by Bjørge-Engeland et al. (2024) demonstrated the feasibility of such an approach by reporting simultaneous TGF observations from both a satellite and an aircraft, highlighting the potential of multi-platform measurements.

Airplanes generally avoid thunderstorms to protect passengers and avoid damage. Furthermore, there are radiation risks associated with flying over TGFs (Dwyer et al., 2010; Tavani et al., 2013; Pallu et al., 2021; Maia et al., 2024). Nevertheless, overcoming these challenges offers a possibility of significantly extending the TGF observations, as was demonstrated in Bowers et al. (2018), Smith et al. (2011), and Østgaard et al. (2024b). The measurements on uncrewed weather balloons are nearly risk-free, and recently it has also been demonstrated that they are feasible for investigation of TGFs (Helmerich et al., 2024).

The recent ALOFT campaign, which used an ER-2 aircraft to fly above thunderstorms in the vicinity of the Gulf of Mexico, is particularly noteworthy. The aircraft flew at an altitude of 20 km and gathered 60 h of flight time, registering 96 TGFs (Østgaard et al., 2024b). These observations, along with the limited findings from earlier airborne efforts (Smith et al., 2011; Bowers et al., 2018), have demonstrated that the number of TGF-producing lightning events is much higher than previously estimated based on satellite data alone. Moreover, these missions have also detected numerous gamma ray glows (Marisaldi et al., 2024) and even revealed a newly observed phenomenon, flickering gamma ray flashes (Østgaard et al., 2024b). Such findings highlight the value of conducting measurements in the vicinity of thunderstorms, particularly from above, where high-quality TGF data can be collected. Building on these successes, future airborne campaigns – whether using research aircraft, regular jet airplanes, or weather balloons – could further expand our understanding of high-energy atmospheric phenomena.

In this paper, we investigate the detectability of TGFs at altitudes reachable by airplanes and weather balloons (5–35 km). We calculate the fluences and energy spectra of various radiation types as a function of TGF altitude of origin and radial distance from the axis of the beam. The calculations are performed by the MCNP-6 Monte Carlo software (Goorley et al., 2013). The results provide estimations of the fluences obtainable by measurements on board aircraft or weather balloons, including the energy spectra. The energy spectra of particles are shown in relation to vertical and radial distance from TGF origin. The results are discussed in regards to the technical constraints for detectors to detect TGFs and the implementability of such measurements on board aircraft or weather balloons. Similar efforts have been made by Hansen et al. (2013) and Ursi et al. (2022), who focused solely on gamma ray particles and the estimation of generated photons. This work extends the analysis to other particle types, such as electrons and neutrons, and also includes the energy spectra of the particles.

2 Materials and methods

TGF Monte Carlo simulations

The simulations were performed using the general-purpose 3D Monte Carlo particle transport simulation tool MCNP6 (Goorley et al., 2013). To estimate the fluences and spatial distributions of particles generated by TGFs at various altitudes, the transport of accelerated particles through the atmosphere was simulated. The calculations were conducted using the NRLMSISE-00 atmosphere model (Picone et al., 2002), with parameters set for 1 January 2022, at a longitude of 15° and three different latitudes: 0, 30, and 60° (representing tropical, temperate, and high-latitude regions, respectively). The model accounts for variations in air composition and density as a function of altitude.

The Monte Carlo model of the atmosphere was constructed up to an altitude of 50 km in discrete steps of 100 m, with different densities and compositions. The air nuclides considered in the model were ^{14}N, ^{16}O, and ^{40}Ar. Water content in the atmosphere was not considered in the calculations. The primary particles used as input in the model were electrons with an energy spectrum calculated by Dwyer and Babich (2011) and can be seen in Fig. 1. This spectrum was derived based on the relativistic runaway electron avalanche theory. The point source emitted the accelerated electrons upward in a vertical direction. The source altitudes were 5 km for a latitude of 60° (high-latitude region), 10 km for a latitude of 30° (temperate region), and 15 km for latitude of 0° (tropical region) (Wallace and Hobbs, 2006). The numbers of primary particles in these calculations were 2.78×10^9, 2.64×10^9, and 2.63×10^9, respectively. These values differ because each simulation was subject to varying compute time limits on a shared computing cluster, where jobs were queued and executed as resources became available. The particles produced from the interactions of primary electrons were scored by various tallies, which are constructs within the MCNP6 software used to record properties of the radiation field (such as fluence and flux) or the radiation itself (such as energy and direction). Properly defining these tallies in the simulation allows for the extraction of meaningful information. In this study, a cylindrical mesh tally of type 1 was used to evaluate fluences, while standard F2 tallies were employed to score the energy spectra of ionizing radiation particles. The results of fluences scored by cylindrical mesh tallies were normalized to 10^{17} particles of primary electrons (> 1 MeV) to estimate the flux for a TGF. Many studies normalize results to the number of observed photons as they can be observed. Such normalization would also make comparisons with other studies more straightforward. However, we chose to normalize to primary electrons because the efficiency of bremsstrahlung production depends on altitude and chemical composition of the air (Groom and Klein, 2000). In denser air, electrons undergo more frequent bremsstrahlung interactions, leading to a higher probability

of gamma ray emission compared to lower-density regions at higher altitudes. Therefore, normalizing to the number of primary electrons provides a more direct way to account for these altitude-dependent effects and to assess the TGF intensity. The results show fluences and the spatial distribution of electrons, photons, and neutrons.

MCNP6 incorporates a comprehensive set of libraries for simulating the interactions of electrons, photons, and neutrons with matter. These include major processes such as Møller scattering, elastic scattering, Compton scattering, pair production, bremsstrahlung, photoelectric absorption, and photonuclear reactions. These libraries provide detailed cross-section data for a wide range of interactions, enabling accurate simulations of electromagnetic radiation transport and particle interactions in the atmosphere. While MCNP6 has not been specifically benchmarked in the studies (Rutjes et al., 2016; Sarria et al., 2018), it is a widely used and well-established tool for Monte Carlo simulations in various research fields. Given that it contains the necessary libraries and interactions, we assume it is an appropriate tool for this type of analysis. The absorption of neutrons in the atmosphere was considered in our analysis. Photonuclear reactions were modeled using established nuclear data libraries, specifically the 7-N-14 and 18-Ar-40 photonuclear reaction data from ENDF/B-VII.0, as well as the O-16 photonuclear data from the LA150 Photonuclear Data Library. These datasets provide cross-sections for photon-induced nuclear reactions relevant to neutron production in the atmosphere.

The energy spectra of particles were tallied during their passage through surfaces at different altitudes. The simulated cylindrical volume (40 km radius and 50 km altitude) was divided into smaller cylinders to allow the segmentation of the tally surfaces (with a segmentation step of 1 km in cylinder radius).

The cylindrical mesh tallies for scoring of particle fluences had a different division than the tally used for scoring the energies of particles. Mesh tallies had radii of 40 km, with steps of 40 m; altitude from 50 m up to 50 km, with steps of 50 m; and one angle, from 0 up to 360°.

The physics settings for the calculation were set such that the production of bremsstrahlung and photonuclear reactions was on. The energy cut-offs for electrons, photons, and neutrons were 10, 10, and 10^{-6} keV, respectively. The Earth's magnetic fields were not considered in the simulations.

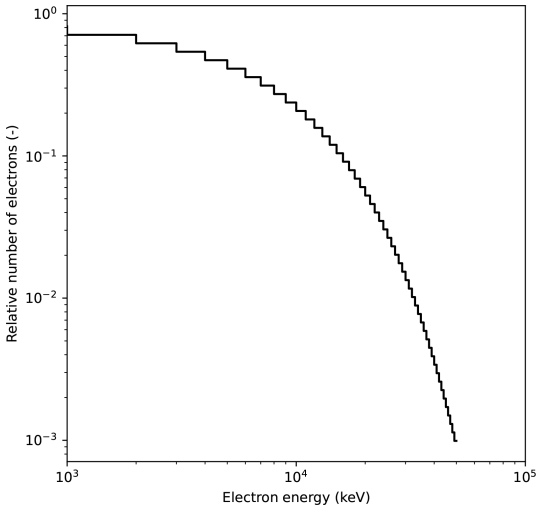

Figure 1. The initial electron spectrum used as primary particles for the simulations.

3 Results

3.1 Photon fluence

The spatial distribution of photon fluences is depicted in Fig. 2. Figure 2 shows fluences for three different altitudes of TGF origin: 5, 10, and 15 km. It can be observed that the photon beam has the shape of a cone. The opening angle of the cones increases with the altitude of the TGF origin. When the altitude of the TGF origin is at 5 km, the fluence of at least 1 cm^{-2} extends up to an altitude of nearly 25 km, with a radial spread of up to 6 km from the origin. For a TGF origin at 10 km, the irradiated cone rapidly elongates and widens; the 1 cm^{-2} threshold region reaches up to an altitude above 50 km (beyond the simulation boundaries) with a maximum radial spread of 1 cm^{-2} isofluence of nearly 20 km. In the case of a TGF at an altitude of 15 km, the region with a fluence higher than 1 cm^{-2} stretches beyond the simulation boundaries of 50 km in altitude and a radial distance of over 40 km. At an altitude of 20–35 km (reachable by weather balloons), the radial distance of the detectability region exceeds 30 km. It can be seen that for narrow geometry the detectability region rapidly broadens at higher altitudes. Another implication is that TGFs originating at higher altitudes can be measured at larger distances. Therefore, platforms such as weather balloons which can climb up to 35 km are more suitable for high-altitude TGFs. It can be seen that the TGF altitude is a crucial parameter influencing the irradiated volume by the bremsstrahlung photons and the beam shape in the observed simulation boundaries. This has significant consequences for all measurements performed above the thunderstorms as it defines the detectability regions together with the brightness of the TGF and its energy spectrum.

Figure 3 shows a comparison of the obtained photon fluences with results published in Hansen et al. (2013). The comparison is not straightforward due to differences in simulation methodologies. In particular, Hansen et al. (2013) directly simulated photon propagation, whereas the present study is based on simulations of electrons, where bremsstrahlung photons are produced as secondary particles. Since the number of generated photons per electron was not explicitly recorded in this work, a scaling factor is required

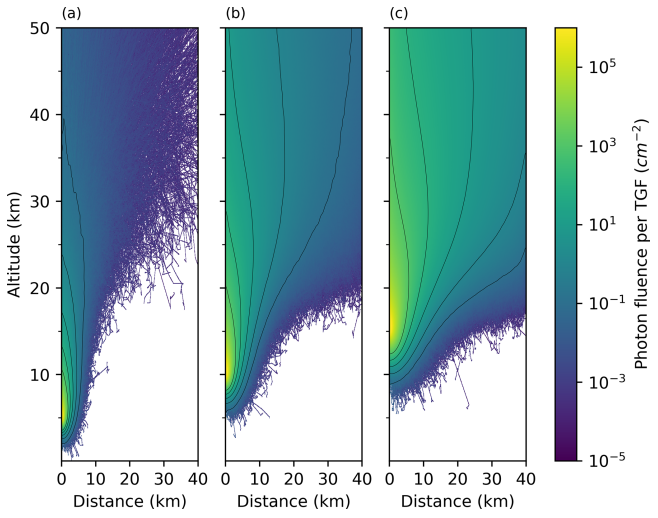

Figure 2. Fluence of photons caused by a TGF at an altitude of **(a)** 5 km, **(b)** 10 km, and **(c)** 15 km. The depicted isofluences show photon fluences of 10^{-1}, 10^{0}, 10^{1}, 10^{2}, and 10^{3} cm^{-2}.

for direct comparison. We refer to this scaling as the electron-to-photon conversion factor, which represents the average number of electrons required to produce one bremsstrahlung photon. Here, we assume that, on average, 10 electrons are needed to produce 1 bremsstrahlung photon. This value was taken from Skeltved et al. (2014) as an upper bound value for TGFs produced in strong electric fields. For weaker electric fields ~ 284 kV m^{-1} the authors estimated the value to be closer to one runaway electron to one bremsstrahlung photon, which would result in better agreement between the comparison.

Another key difference lies in the energy thresholds considered in the simulations. Hansen et al. (2013) only accounted for photons with energies above 300 keV, while the present study includes photons down to 10 keV. This distinction leads to differences in the total fluence values, as lower-energy photons contribute significantly to the overall photon population. Additionally, the beaming geometries differ: the present study employs a narrow beam geometry, whereas Hansen et al. (2013) used a wider beam. These factors collectively influence the observed fluence distributions and must be taken into account when comparing results.

The photon energy spectra were recovered for various radial distances from the TGF origin. Figure 4 shows the energy spectra of photons at three different altitudes – 25, 20, and 15 km, – as a function of radial distance from the axis of the TGF originating at an altitude of 10 km. It can be seen that for various radial distances, the ratio between low-energy (< 100 KeV) and high-energy (> 1 MeV) components changes. The high-energy component is more substantial near the axis of the TGF. It can also be observed that the maximum energy of photons decreases as the radial distance increases. Hence, there is a softening of the gamma ray energy spectra at the edges of the irradiated cones. This effect has been observed by Gjesteland et al. (2011) and Lindanger et al. (2021). This effect is especially pronounced at higher altitudes. To better visualize and analyze the spectral hardness, Fig. 5 shows the normalized energy spectra of photons (normalization to its maximum). By normalizing the spectra, the change in the ratio between low-energy (< 100 keV) and high-energy (> 1 MeV) components becomes more apparent. This normalization highlights the softening of the gamma ray energy spectra at the edges of the irradiated cones. The calculated figures of merit, defined as the ratio of low-energy to high-energy gamma rays, are 34.9, 50.95, 88.39, 237.74, and 1649.85 for radial distance ranges of 0–2, 2–5, 5–10, 10–20, and 20–40 km, respectively, indicating progressively softer spectra with increasing distance. Notably, immediately above the TGF, a distinct sharp edge appears in the energy spectrum (approximately at 50 MeV), which corresponds to the maximum energy of primary electrons. However, at a higher radial distance from the center of the TGF, this sharp edge moves to lower energies. The visible peak between 497–599 keV is caused by 511 keV photons from the annihilation of positrons. The positrons are created mainly by the pair production of high-energy photons. The energy interval of 497–599 keV corresponds to the bin size of the tally used to score the energy spectrum; the true energy of the annihilation photons is 511 keV. The 511 keV peak is more pronounced at higher altitudes and at distances closer to the axis of the TGF. To quantify the annihilation peak we calculated the equivalent width of the peak for a detection altitude of 25 km and an altitude of TGF origin of 10 km. The resulting equivalent widths are 0.16, 0.15, 0.13, 0.11, and 0.08 MeV for radial distances of 0–2, 2–5, 5–10, 10–20, and 20–40 km, respectively. The equivalent width is a measure used to quantify the strength of a spectral line or peak. It represents the width of a feature in a spectrum, normalized by the intensity of the peak itself.

These features of the photon energy spectrum (softening of the beam at the edges and the presence of a 511 keV peak) could be used for estimating the radial distance to the TGF axis. This method may have limited practical use because it requires detecting a large number of photons, which is especially challenging for small detectors.

3.2 Electron fluence

The spatial distribution of electron fluences is depicted in Fig. 6. Figure 6 shows fluences for three different altitudes of TGF origin: 5, 10, and 15 km. The spatial distribution of electrons is similar to the photon distribution, as most of the electrons are created by interactions of gamma rays with atoms in the atmosphere. Nevertheless, electron fluences have some specific characteristics. One of these characteristics of the electron fluence distribution is the presence of long tracks of individual high-energy electrons that are created by interactions of gamma rays with the atmosphere. These tracks are

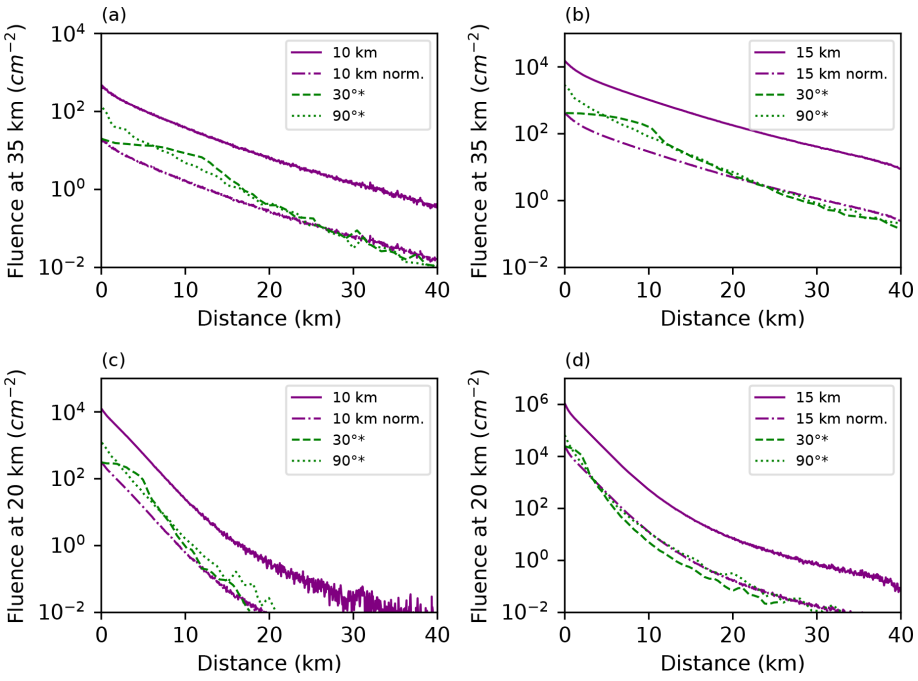

Figure 3. Fluence of photons compared with results in Hansen et al. (2013) – TGF altitude of 10 and 15 km with two beaming geometries of 30 and 90°. Dash-dotted lines show results from Hansen et al. (2013) for beaming geometries of 30 and 90°, respectively. Solid lines show results of the presented study using an electron-to-photon conversion factor of 10. The dash-dotted line represents results normalized to the maximum fluence for a geometry of 30°. Panel **(a)** shows the fluence at an altitude of 35 km and TGF origin of 10 km, panel **(b)** shows the fluence at an altitude of 35 km and TGF origin of 15 km, panel **(c)** shows the fluence at an altitude of 20 km and TGF origin of 10 km, and panel **(d)** shows the fluence at an altitude of 20 km and TGF origin of 15 km.

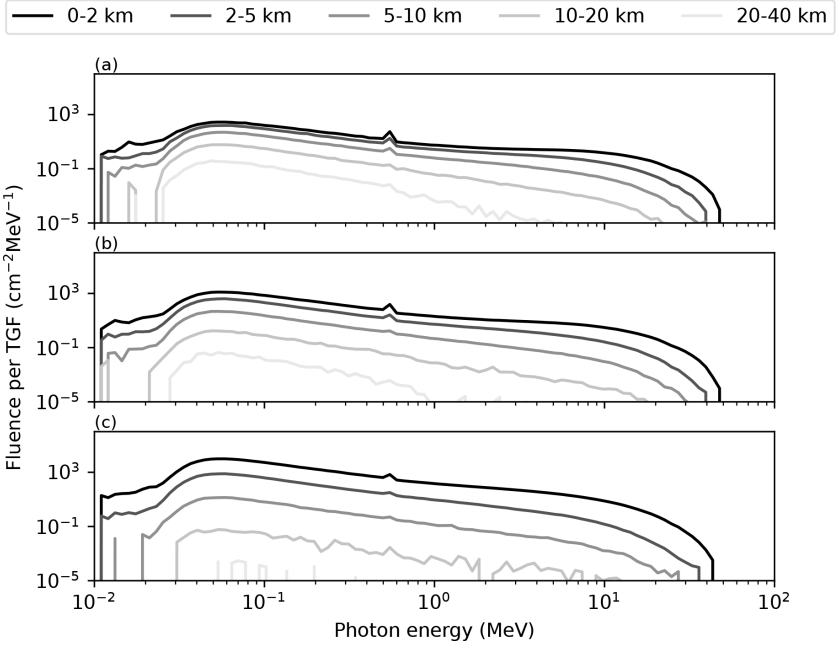

Figure 4. Energy spectra of photons caused by a TGF at different radial distances from the TGF origin. The altitude of the TGF origin is 10 km, and the energy spectra are recorded at altitudes of **(a)** 25 km, **(b)** 20 km, and **(c)** 15 km.

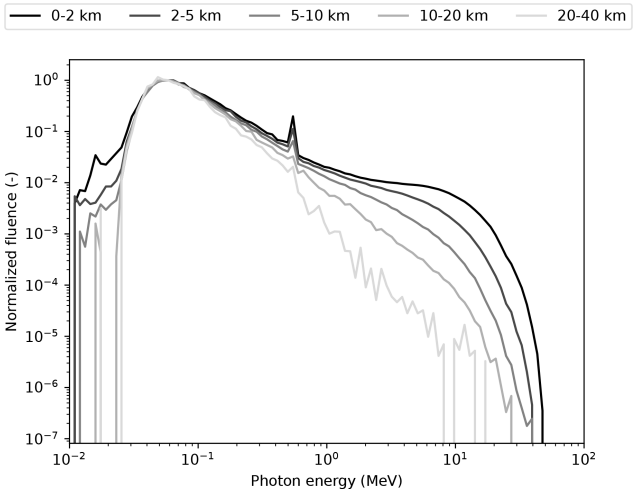

Figure 5. Normalized energy spectra of photons measured at an altitude of 25 km. Normalization is performed on the fluence maxima. The altitude of the TGF origin is 15 km.

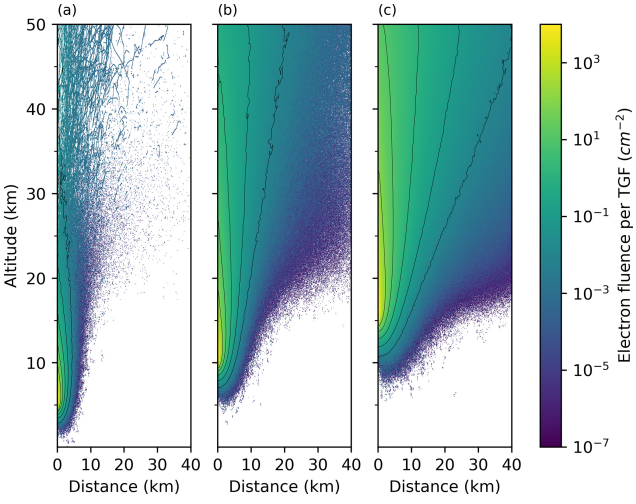

Figure 6. Fluence of electrons caused by a TGF at an altitude of **(a)** 5 km, **(b)** 10 km, and **(c)** 15 km. The depicted isofluences show electron fluences of 10^{-2}, 10^{-1}, 10^{0}, 10^{1}, and 10^{2} cm^{-2}.

visible in the high-altitude section (a), showing TGFs with an origin at 5 km. Such electrons have large energies and can travel significant distances in the air. Another characteristic is that the largest fluences are located in smaller and narrower cones than those observed for gamma rays. To highlight these differences, the profiles of photons and electrons and the electron-to-photon ratio are plotted in Fig. 7 for two fixed altitudes. It can be seen that as the viewer moves further away from the central axis of the TGF the number of electrons to photons quickly decreases and then stabilizes at a value near zero.

The energy spectra of electrons caused by a TGF at different radial distances are shown in Fig. 8. Similar to photons, the high-energy part of the electron energy spectrum is focused mainly around the center of the TGF, whereas on the edges of the cone, the energy spectrum softens. Although the overall number of electrons decreases as they move to higher altitudes, the shapes of the energy spectra do not undergo significant changes and remain relatively stable.

Figure 9 also presents a comparison between our simulated electron energy spectra at an altitude of 50 km (TGF altitude of 15 km) and the spectra of escaped electrons from the Earth's atmosphere performed by Dwyer et al. (2008). To enable a meaningful comparison, our spectrum was normalized such that its integral matches that of Dwyer's within the energy range covered by their data. Because the energy axis is logarithmic, the counts were first multiplied by the corresponding bin widths before integration. Although our spectrum extends to slightly lower energies, this extended portion was excluded from the normalization integral but retained in the final plot with the same normalization factor applied. The results show good agreement, indicating that our simulation reliably captures the energy distribution of scattered electrons. This agreement also serves as a validation of our approach, as the simulations of Dwyer et al. (2008) were conducted under similar conditions, particularly in terms of the beaming geometry.

3.3 Neutron fluence

The spatial distribution of neutron fluences is depicted in Fig. 10. Figure 10 shows fluences for three different altitudes of TGF origin: 5, 10, and 15 km. Neutrons are generated by photonuclear reactions of high-energy gamma rays with atoms of the atmosphere. These reactions have low cross-sections; therefore, the resulting neutron fluences are lower than those of gamma rays or electrons. Moreover, the regions with sufficient neutron fluences (at least 1 cm^{-2}) are relatively small compared to those of electrons and photons. For these reasons, photoneutrons are likely to be missed, or their contribution in the detector would be insignificant. Nevertheless, the absence of detected neutrons can still be valuable for estimating the minimal distance between the radiation source and the detector.

The energy spectra for two different radii are shown in Fig. 11. It can be seen that neutron energy spectra are very insensitive to the radial distance from the axis of the TGF and altitude where it is scored. Carlson et al. (2010) also report that the neutron energy spectra produced in TGFs are largely composed of thermal neutrons, with only a small fraction of high-energy neutrons. Additionally, they find that the neutron energy spectra are insensitive to the altitude at which they were tallied, echoing our results where neutron energy spectra do not show significant dependence on altitude. However, the low statistics cause the energy spectra to exhibit noise.

It is important to note that while the spatial and energy distributions of neutrons have been analyzed in this study, the timing of neutron production and their arrival at detectors

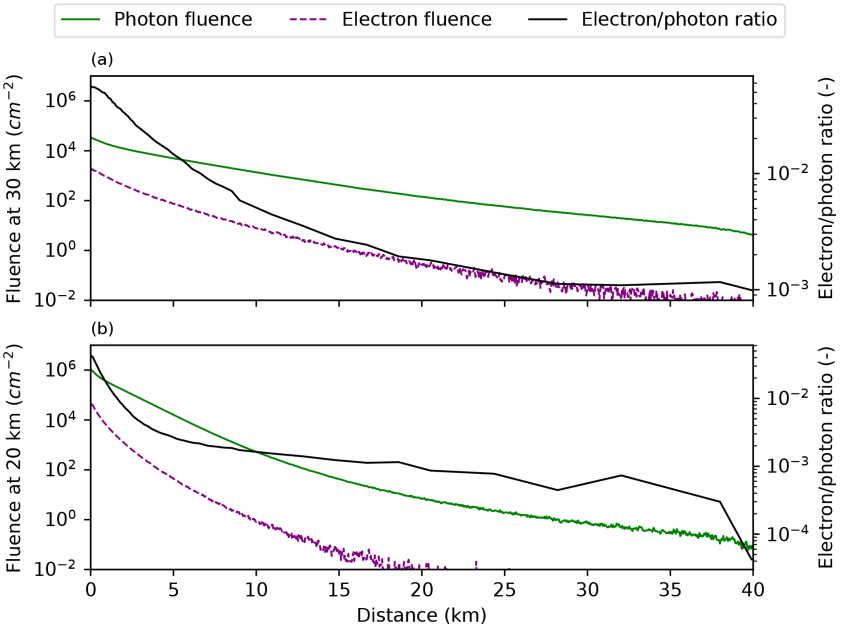

Figure 7. Profiles of photon and electron fluences at two fixed altitudes of **(a)** 30 km and **(b)** 20 km. The altitude of TGF is 15 km. The ratio of electrons to photons is also plotted.

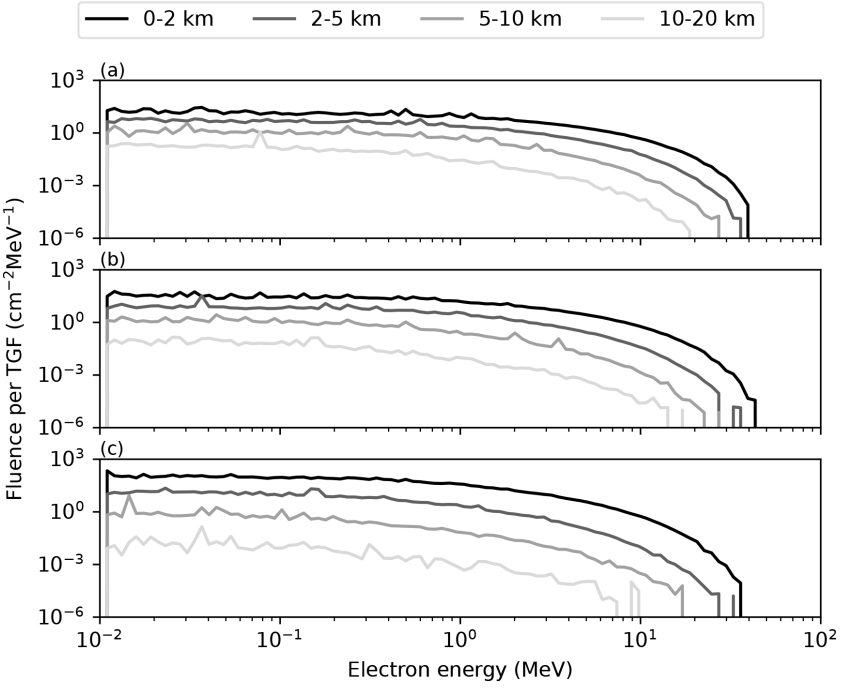

Figure 8. Energy spectra of electrons caused by a TGF for different radial distances from the TGF origin. The altitude of the TGF origin is 15 km, and energy spectra are recovered from altitudes of **(a)** 30 km, **(b)** 25 km, and **(c)** 20 km.

was not included in the simulations. As such, the temporal characteristics of neutron emissions such as their reduction in speed in the atmosphere or the time distribution of their arrival are not addressed here. Future studies could incorporate timing analysis to explore these factors, which would provide a more complete understanding of the neutron dynamics in relation to TGF events.

There are other studies (Rutjes et al., 2017; Wada et al., 2020) that are related to the current work, but due to key differences in focus and methodology, direct comparison is

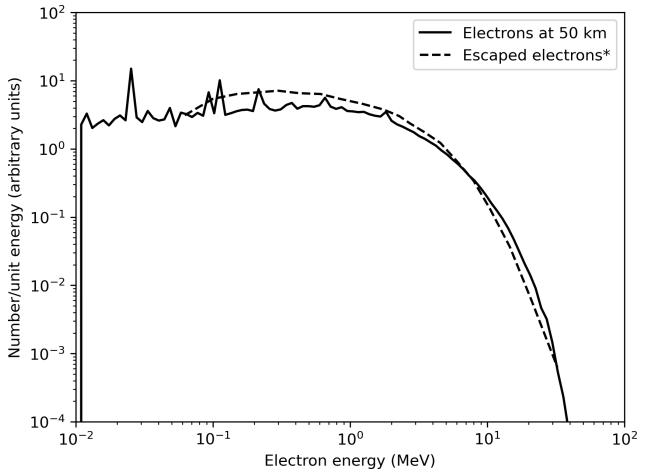

Figure 9. A comparison of simulated electron energy spectra at an altitude of 50 km (TGF altitude of 15 km) and the spectra of escaped electrons from the simulations performed by Dwyer et al. (2008).

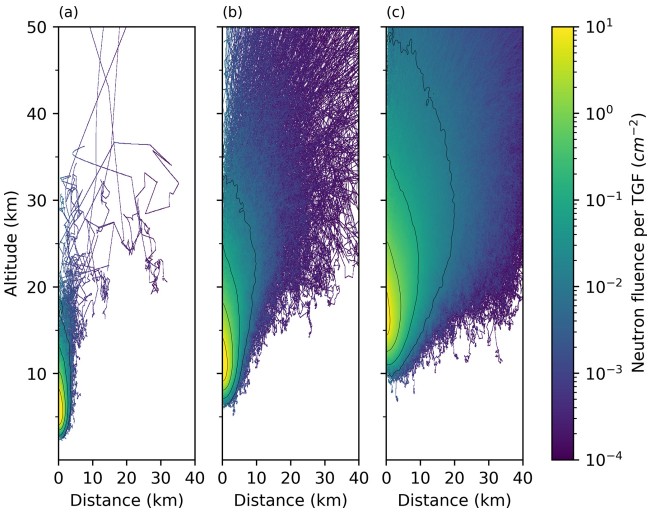

Figure 10. Fluence of neutrons caused by a TGF at an altitude of **(a)** 5 km, **(b)** 10 km, and **(c)** 15 km. The depicted isofluences show neutron fluences of 10^{-2}, 10^{-1}, 10^{0}, and 10^{1} cm^{-2}.

not feasible. Rutjes et al. (2017) examine afterglows produced by neutrons some time after the TGF event. However, the present work only considers neutrons generated during the TGF itself and does not include time scoring, making this type of afterglow analysis outside the scope of the current research. Wada et al. (2020) present simulations of downward TGFs and measures of neutron spectra at ground level, which includes thermalization of neutrons upon reaching the Earth's surface. In contrast, the present work focuses on upward TGFs and neutron propagation at altitudes relevant to balloon and aircraft measurements. Therefore, any direct comparison would be difficult to justify.

4 Discussion

The MCNP6 calculations reveal the distribution of fluences of various particles caused by vertical TGFs and their energy spectra at different altitudes and radial distances from the TGF axis. The calculations focus mainly on TGF characteristics at altitudes of 0–50 km, where only a few measurements have been performed so far. Such measurements could provide valuable additional information about TGFs and address the limitations of satellite-based observations. However, there are several significant challenges remaining, including delivering detectors to these high altitudes above thunderstorms and designing detectors to maximize the amount of information obtained.

4.1 Means of transportation

The obvious option is to use airplanes, which are easily maneuverable, can stay airborne for a long period, and can reach relatively high altitudes of 12–13 km. Since the cumulonimbus clouds at the top of the thunderstorm in tropical regions are around 18 km, this might not always be sufficient to fly above the thunderstorm. However, it could be adequate for temperate and high-latitude regions where the tops of the clouds are at altitudes of 13 km and 8 km, respectively (Wallace and Hobbs, 2006). Another possibility for using aircraft is during winter thunderstorms, when thunderstorms typically reach altitudes of only several kilometers in temperate regions (Popová et al., 2023; Kolmašová et al., 2022). The advantage of winter thunderstorms is also the possibility of performing various mutual radiation measurements on the ground (Wada et al., 2019; Enoto et al., 2017). The drawback of using aircraft for observing winter thunderstorms is that the detectors need to be located relatively close radially to the axis of the TGF, as shown in Figs. 2, 6, and 10. Hence, the TGF might miss the detectors even when the aircraft is in the vicinity of an active thunderstorm. Additionally, there are radiation risks to the aircraft and crew, which might be significant, particularly in the immediate vicinity (400 m) of the avalanche region, as noted by Pallu et al. (2021). However, outside of this region, the radiation risk is considerably lower. It is also important to note that pilots generally avoid flying directly over low-altitude thunderstorms due to the potential for turbulence and other safety concerns, as this presents a greater risk to flight operations. To avoid the most severe radiation effects of the TGFs, the plane should always stay out of reach of the primarily accelerated electrons (Dwyer et al., 2010; Pallu et al., 2021).

The potential of using planes for TGF research was demonstrated by the ALOFT campaign, which measured a large number of TGFs (Ostgaard et al., 2024a) when the NASA-owned ER-2 aircraft, flying at an altitude of approximately 20 km, was positioned above thunderstorms. Another option is to use weather balloons as carriers of detectors. Weather balloons are usually filled with helium and can as-

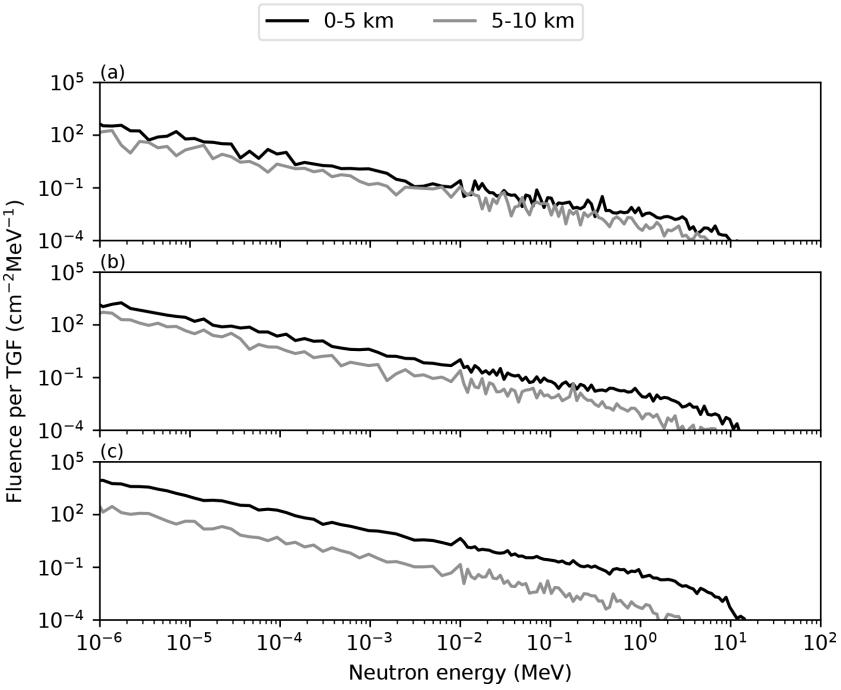

Figure 11. Energy spectra of neutrons caused by a TGF for different radial distances from the TGF origin. The altitude of the TGF origin is 10 km, and the energy spectra are recovered from altitudes of **(a)** 25 km, **(b)** 20 km, and **(c)** 15 km.

cend up to 35 km, but they cannot be maneuvered, their payload mass is limited, and their use is usually strictly regulated by law. For these reasons, it would likely be difficult to use weather balloons for tracking TGFs above thunderstorms. Nevertheless, measurements with weather balloons would have the advantage of being able to fly above the cloud tops of even the tallest thunderstorms (summer thunderstorms in temperate and tropical regions). Hence, TGFs could be detected at larger radial distances from the TGF axis than for TGFs originating at lower altitudes, as is shown in Figs. 2, 6, and 10. When weather balloons are launched, they drift with the wind. Although there are online tools for predicting the weather balloon trajectory, it would be very challenging to time the launch so that it flies over a fast-moving, active thunderstorm cell. This would require in-depth experience and expertise in meteorology, weather forecasting, and weather balloon launching. The last suggested option is the use of high-altitude platform stations (HAPSs), which could combine the advantages of aircraft and weather balloons, as some HAPS concepts offer the capability to ascend to altitudes of 20 km while also providing maneuverability and a large payload capacity (Gonzalo et al., 2018). The disadvantage of HAPSs is that they are not currently widely available.

4.2 Detectors

It was shown that the fluxes and energies of different particle types vary significantly based on the location of the TGF origin, its brightness, and the measurement location. Other variables influencing the fluxes and particle energies include the energy spectrum of the primary electrons and the tilt of the TGF. We have only considered TGFs with an upward direction, one energy spectrum, and one brightness. These variables also change, as described above, and therefore, the calculated particle fluxes originating from TGFs should be considered to be estimates. Nevertheless, these estimates should be sufficient to define the properties of ionizing radiation detectors for TGF detection.

The most significant component of the TGF is bremsstrahlung, which has the largest reach and is relatively easy to detect with various ionizing radiation detectors. The most commonly used detectors are scintillators because of their large volumes and high density. Reasonably expected fluences of gamma rays might reach values up to 1000 cm^{-2} per TGF (Fig. 2) for the simulated conditions, whereas the background fluence of cosmic ray photons is around 30 cm^{-2} s^{-1} at an altitude of 20 km and in central Europe. Since the TGF consists of sub-millisecond pulses, during which a large number of particles are created, the TGF signal can exceed the background by several folds. Sometimes, the bursts are so intense that scintillator detectors become saturated (Tran et al., 2015) as the decay of the signal takes hundreds of nanoseconds. In such cases, it is not possible to distinguish individual gamma rays, and information about gamma ray energy and intensity is either lost or diminished. This can be mitigated by using scintillators with faster signal decay times and lower light yield, decreasing the

size of the scintillator, or using shielding of the detection element. In general, such precautions reduce the sensitivity of the detector to gamma rays, enabling it to measure high-intensity TGFs. On the other hand, insensitive detectors would not detect TGFs that are farther away or have different energy spectra. Therefore, a combination of gamma ray detectors with various sensitivities would be an effective approach to ensure that energy and intensity information can be recovered from the measurements, as demonstrated in previous TGF detection campaigns such as ADELE (Smith et al., 2011; Bowers et al., 2018) and ALOFT (Kochkin et al., 2021; Ostgaard et al., 2024a; Østgaard et al., 2024b), where multi-detector setups were used to mitigate saturation effects and improve spectral reconstruction. Moreover, the energy spectrum can be estimated by analyzing the response of several detectors with different sensitivities to different energies. Such a TGF detector assembly could be similar to a detector used for spectrometry of pulsed radiation fields generated by high-power lasers (Stránský et al., 2021).

The second particle type of interest is electrons, which are likely to be detected in the presence of stronger gamma radiation fields. Reasonably expected fluences of electrons from TGFs are up to $100\,\mathrm{cm}^{-2}$ for the simulated conditions, while the background fluence of electrons and positrons is around $2.5\,\mathrm{cm}^{-2}\,\mathrm{s}^{-1}$. For electron detection, a detector with a smaller volume can be used, as electrons directly interact with matter by ionizing it. Therefore, pixel or strip semiconductor detectors or diode-based detectors are suitable because their detection efficiency is much higher than for gamma rays. The advantage of such detectors is that they can be used in a telescopic configuration (multiple diodes), allowing estimation of the incident angle of the electrons if they traverse multiple layers of semiconductor. However, this method is primarily effective for high-energy electrons, which constitute only a small fraction of the total electron population. If the diodes have a sufficient volume, the telescope can also function as a calorimeter and provide information about the energy of incident electrons. A limiting factor for semiconductor diodes might be their size, as scaling diode volume is not straightforward. Therefore, detecting low fluxes of electrons with diodes could be challenging and might require an alternative approach, such as using large-surface scintillators. In a calorimetric configuration, the width of diodes would also be a limiting factor. The energy spectrum of electrons ranges from several kiloelectronvolts up to dozens of megaelectronvolts, which would require several millimeters of semiconductor material to fully stop such energetic electrons. If such detectors are placed on an aircraft, the aircraft skin would likely stop the electrons. Therefore, it might be reasonable to use telescopes in weather balloons instead, since the gondolas of such balloons are typically made of light-weight, low-density insulators (e.g., polystyrene), which would not decelerate the electrons significantly. The gondolas can also be designed so that there is a minimum amount of material to shield the electron detectors.

Another component of interest is neutrons. The production of neutrons by photonuclear reactions is inefficient, and the neutron fluxes are relatively low, even in the proximity of the TGF origin (Fig. 10). Moreover, the cross-sections of neutron interactions with matter are relatively low, so neutron detectors need to be large to obtain useful information about TGFs. This makes them suitable only for platforms that can carry large payloads, such as aircraft. The neutron energies range from millielectronvolts up to megaelectronvolts, as shown in Fig. 11. Hence, TGF neutron detectors should measure over a very broad range of energies. A key challenge for neutron detectors is selectivity, as they are immersed in a much larger photon flux. Therefore, these detectors must be significantly more sensitive to neutrons than to photons, or the detectors must differentiate between photons, electrons, and neutrons. One of the possible methods is to use pulse shape discrimination, as was demonstrated in Pallu et al. (2023).

5 Conclusions

The measurements of TGFs performed directly above the thunderstorms could help overcome the challenges faced by satellites, namely the attenuation of gamma rays by the atmosphere and large distance between TGF source and detectors. Large distances between the TGF origin and detectors on board satellites cause low statistics of detected gamma rays and blurring of the time structure of TGFs. The measurement campaign with aircraft, weather balloons, or HAPSs could provide valuable information about the occurrence of TGFs under various conditions (latitude, lightning, and thunderstorm types) and could resolve the time structure of TGFs with much better accuracy. The findings discussed in previous sections should serve as a study showing the expected fluences, energies, and ranges of ionizing radiation generated by TGFs on board aircraft and weather balloons. The main findings can be summarized into three points:

1. Estimated fluences of TGF photons measured on board aircraft or weather balloons could reach up to 1000 and $100\,\mathrm{cm}^{-2}$ for electrons, for a brightness of 10^{17} primary electrons (> 1 MeV). On the other hand, the fluences of neutrons are very low, up to $1\,\mathrm{cm}^{-2}$.

2. TGFs originating at low altitudes have much narrower beams than TGFs originating at higher altitudes. Therefore, the use of weather balloons for the detection of TGFs might be more suitable for high-altitude thunderstorms, such as summer thunderstorms.

3. Features in photon and electron energy spectra, such as maximum energy, ratios between low- and high-energy particles, and the presence of 511 keV photons, can be used to estimate the radial distance from the axis of the TGF.

Data availability. All raw data can be provided by the corresponding authors upon request. The data are available at https://doi.org/10.6084/m9.figshare.28612058.v1 (Sommer, 2025).

Author contributions. MS and TC performed the Monte Carlo simulations. MS wrote the manuscript draft. IA, MK, OV, and OP reviewed and edited the manuscript.

Competing interests. The contact author has declared that none of the authors has any competing interests.

Disclaimer. Publisher's note: Copernicus Publications remains neutral with regard to jurisdictional claims made in the text, published maps, institutional affiliations, or any other geographical representation in this paper. While Copernicus Publications makes every effort to include appropriate place names, the final responsibility lies with the authors.

Financial support. This research has been supported by the Ministerstvo Školství, Mládeže a Tělovýchovy (grant no. CZ.02.1.01/0.0/0.0/15_003/0000481).

Review statement. This paper was edited by Markus Rapp and reviewed by Yuuki Wada and one anonymous referee.

References

Belz, J., Krehbiel, P., Remington, J., Stanley, M., Abbasi, R., LeVon, R., Rison, W., Rodeheffer, D., Abu-Zayyad, T., Allen, M., Barcikowski, E., Bergman, D., Blake, S., Byrne, M., Cady, R., Cheon, B., Chikawa, M., di Matteo, A., Fujii, T., Fujita, K., Fujiwara, R., Fukushima, M., Furlich, G., Hanlon, W., Hayashi, M., Hayashi, Y., Hayashida, N., Hibino, K., Honda, K., Ikeda, D., Inadomi, T., Inoue, N., Ishii, T., Ito, H., Ivanov, D., Iwakura, H., Jeong, H., Jeong, S., Jui, C., Kadota, K., Kakimoto, F., O, K., K, K., Kasami, S., Kawai, H., Kawakami, S., Kawata, K., Kido, E., Kim, H., Kim, J., Kim, J., Kuzmin, V., Kuznetsov, M., Kwon, Y., Lee, K., Lubsandorzhiev, B., Lundquist, J., Machida, K., Matsumiya, H., Matthews, J., Matuyama, T., Mayta, R., Minamino, M., Mukai, K., Myers, I., Nagataki, S., Nakai, K., Nakamura, R., Nakamura, T., Nakamura, Y., Nonaka, T., Oda, H., Ogio, S., Ohnishi, M., Ohoka, H., Oku, Y., Okuda, T., Omura, Y., Ono, M., Oshima, A., Ozawa, S., Park, I., Potts, M., Pshirkov, M., Rodriguez, D., Rubtsov, G., Ryu, D., Sagawa, H., Sahara, R., Saito, K., Saito, Y., Sakaki, N., Sako, T., Sakurai, N., Sano, K., Seki, T., Sekino, K., Shibata, F., Shibata, T., Shimodaira, H., Shin, B., Shin, H., Smith, J., Sokolsky, P., Sone, N., Stokes, B., Stroman, T., Takagi, Y., Takahashi, Y., Takeda, M., Takeishi, R., Taketa, A., Takita, M., Tameda, Y., Tanaka, K., Tanaka, M., Tanoue, Y., Thomas, S., Thomson, G., Tinyakov, P., Tkachev, I., Tokuno, H., Tomida, T., Troitsky, S., Tsunesada, Y., Uchihori, Y., Udo, S., Uehama, T., Urban, F., Wallace, M., Wong, T., Yamamoto, M., Yamaoka, H., Yamazaki, K., Yashiro, K., Yosei, M., Yoshii, H., Zhezher, Y., and Zundel, Z.: Observations of the origin of downward terrestrial gamma-ray flashes, J. Geophys. Res.-Atmos., 125, e2019JD031940, https://doi.org/10.1029/2019JD031940, 2020.

Bjørge-Engeland, I., Østgaard, N., Sarria, D., Marisaldi, M., Mezentsev, A., Fuglestad, A., Lehtinen, N., Grove, J. E., Shy, D., Lang, T., Quick, M., Christian, H., Schultz, C., Blakeslee, R., Adams, I., Kroodsma, R., Heymsfield, G., Ullaland, K., Yang, S., Hasan Qureshi, B., Søndergaard, J., Husa, B., Walker, D., Bateman, M., Mach, D., Bitzer, P., Fullekrug, M., Cohen, M., Stanley, M., Cummer, S., Montanya, J., Pazos, M., Velosa, C., van der Velde, O., Pu, Y., Krehbiel, P., Roncancio, J., Lopez, J., Urbani, M., Santos, A., Neubert, T., and Gordillo-Vazquez, F.: Evidence of a new population of weak Terrestrial Gamma-Ray flashes observed from aircraft altitude, Geophys. Res. Lett., 51, e2024GL110395, https://doi.org/10.1029/2024GL110395, 2024.

Bowers, G., Smith, D., Kelley, N., Martinez-McKinney, G., Cummer, S., Dwyer, J., Heckman, S., Holzworth, R., Marks, F., Reasor, P., Gamache, J., Dunion, J., Richards, T., and Rassoul, H.: A terrestrial gamma-ray flash inside the eyewall of hurricane Patricia, J. Geophys. Res.-Atmos., 123, 4977–4987, https://doi.org/10.1029/2017JD027771, 2018.

Briggs, M. S., Fishman, G., Connaughton, V., Bhat, P., Paciesas, W., Preece, R., Wilson-Hodge, C., Chaplin, V., Kippen, R., Von Kienlin, A., Meegan, C., Bissaldi, E., Dwyer, J., Smith, D., Holzworth, R., Grove, J., and Chekhtman, A.: First results on terrestrial gamma ray flashes from the Fermi Gamma-ray Burst Monitor, J. Geophys. Res.-Space, 115, A07323, https://doi.org/10.1029/2009JA015242, 2010.

Briggs, M. S., Xiong, S., Connaughton, V., Tierney, D., Fitzpatrick, G., Foley, S., Grove, J. E., Chekhtman, A., Gibby, M., Fishman, G. J., McBreen, S., Chaplin, V., Guiriec, S., Layden, E., Bhat, P., Hughes, M., Greiner, J., Kienlin, A., Kippen, R., Meegan, C., Paciesas, W., Preece, R., Wilson-Hodge, C., Holzworth, R., and Hutchins, M.: Terrestrial gamma-ray flashes in the Fermi era: Improved observations and analysis methods, J. Geophys. Res.-Space, 118, 3805–3830, https://doi.org/10.1002/jgra.50205, 2013.

Carlson, B., Lehtinen, N. G., and Inan, U. S.: Neutron production in terrestrial gamma ray flashes, J. Geophys. Res.-Space, 115, A00E19, https://doi.org/10.1029/2009JA014696, 2010.

Celestin, S. and Pasko, V. P.: Energy and fluxes of thermal runaway electrons produced by exponential growth of streamers during the stepping of lightning leaders and in transient luminous events, J. Geophys. Res.-Space, 116, A03315, https://doi.org/10.1029/2010JA016260, 2011.

Celestin, S., Xu, W., and Pasko, V. P.: Variability in fluence and spectrum of high-energy photon bursts produced by lightning leaders, J. Geophys. Res.-Space, 120, 10–712, https://doi.org/10.1002/2015JA021410, 2015.

Cummer, S. A., Lu, G., Briggs, M. S., Connaughton, V., Xiong, S., Fishman, G. J., and Dwyer, J. R.: The lightning-TGF relationship on microsecond timescales, Geophys. Res. Lett., 38, L14810, https://doi.org/10.1029/2011GL048099, 2011.

Cummer, S. A., Lyu, F., Briggs, M. S., Fitzpatrick, G., Roberts, O. J., and Dwyer, J. R.: Lightning leader altitude progression in terrestrial gamma-ray flashes, Geophys. Res. Lett., 42, 7792–7798, https://doi.org/10.1002/2015GL065228, 2015.

Dwyer, J.: A fundamental limit on electric fields in air, Geophys. Res. Lett., 30, 2055, https://doi.org/10.1029/2003GL017781, 2003.

Dwyer, J., Rassoul, H., Al-Dayeh, M., Caraway, L., Wright, B., Chrest, A., Uman, M., Rakov, V., Rambo, K., Jordan, D., Jerauld, J., and Smyth, C.: A ground level gamma-ray burst observed in association with rocket-triggered lightning, Geophys. Res. Lett., 31, L05119, https://doi.org/10.1029/2003GL018771, 2004.

Dwyer, J., Smith, D., Uman, M., Saleh, Z., Grefenstette, B., Hazelton, B., and Rassoul, H.: Estimation of the fluence of high-energy electron bursts produced by thunderclouds and the resulting radiation doses received in aircraft, J. Geophys. Res.-Atmos., 115, D09206, https://doi.org/10.1029/2009JD012039, 2010.

Dwyer, J. R.: Source mechanisms of terrestrial gamma-ray flashes, J. Geophys. Res.-Atmos., 113, D10103, https://doi.org/10.1029/2007JD009248, 2008.

Dwyer, J. R. and Babich, L. P.: Low-energy electron production by relativistic runaway electron avalanches in air, J. Geophys. Res.-Space, 116, A09301, https://doi.org/10.1029/2011JA016494, 2011.

Dwyer, J. R. and Smith, D. M.: A comparison between Monte Carlo simulations of runaway breakdown and terrestrial gamma-ray flash observations, Geophys. Res. Lett., 32, L22804, https://doi.org/10.1029/2005GL023848, 2005.

Dwyer, J. R., Grefenstette, B. W., and Smith, D. M.: High-energy electron beams launched into space by thunderstorms, Geophys. Res. Lett., 35, L02815, https://doi.org/10.1029/2007GL032430, 2008.

Enoto, T., Wada, Y., Furuta, Y., Nakazawa, K., Yuasa, T., Okuda, K., Makishima, K., Sato, M., Sato, Y., Nakano, T., Umemoto, D., and Tsuchiya, H.: Photonuclear reactions triggered by lightning discharge, Nature, 551, 481–484, https://doi.org/10.1038/nature24630, 2017.

Fishman, G. J., Bhat, P., Mallozzi, R., Horack, J., Koshut, T., Kouveliotou, C., Pendleton, G., Meegan, C., Wilson, R., Paciesas, W., Goodman, S., and Christian, H.: Discovery of intense gamma-ray flashes of atmospheric origin, Science, 264, 1313–1316, https://doi.org/10.1126/science.264.5163.1313, 1994.

Gjesteland, T., Østgaard, N., Collier, A., Carlson, B., Cohen, M., and Lehtinen, N.: Confining the angular distribution of terrestrial gamma ray flash emission, J. Geophys. Res.-Space, 116, A11313, https://doi.org/10.1029/2011JA016716, 2011.

Gjesteland, T., Østgaard, N., Laviola, S., Miglietta, M., Arnone, E., Marisaldi, M., Fuschino, F., Collier, A. B., Fabró, F., and Montanya, J.: Observation of intrinsically bright terrestrial gamma ray flashes from the Mediterranean basin, J. Geophys. Res.-Atmos., 120, 12–143, https://doi.org/10.1002/2015JD023704, 2015.

Gonzalo, J., López, D., Domínguez, D., García, A., and Escapa, A.: On the capabilities and limitations of high altitude pseudo-satellites, Prog. Aerosp. Sci., 98, 37–56, https://doi.org/10.1016/j.paerosci.2018.03.006, 2018.

Goorley, J. T., James, M. R., Booth, T. E., Brown, F. B., Bull, J. S., Cox, L. J., Durkee Jr, J. W., Elson, J. S., Fensin, M. L., Forster III, R. A., Hendricks, J. S., Hughes, H. G. I., Johns, R. C., Kiedrowski, B. C., Martz, R. L., Mashnik, S. G., McKinney, G. W., Pelowitz, D. B., Prael, R. E., Sweezy, J. E., Waters, L. S., Wilcox, T., and Zukaitis, A. J.: Initial MCNP6 release overview-MCNP6 version 1.0, Tech. rep., Los Alamos National Lab.(LANL), Los Alamos, NM (United States), https://doi.org/10.2172/1086758, 2013.

Grefenstette, B. W., Smith, D. M., Hazelton, B., and Lopez, L.: First RHESSI terrestrial gamma ray flash catalog, J. Geophys. Res.-Space, 114, A02314, https://doi.org/10.1029/2008JA013721, 2009.

Groom, D. E. and Klein, S. R.: Passage of particles through matter, Eur. Phys. J. C, 15, 163–173, https://doi.org/10.1007/BF02683419, 2000.

Hansen, R., Østgaard, N., Gjesteland, T., and Carlson, B.: How simulated fluence of photons from terrestrial gamma ray flashes at aircraft and balloon altitudes depends on initial parameters, J. Geophys. Res.-Space, 118, 2333–2339, https://doi.org/10.1002/jgra.50143, 2013.

Hare, B., Uman, M., Dwyer, J., Jordan, D., Biggerstaff, M., Caicedo, J., Carvalho, F., Wilkes, R., Kotovsky, D., Gamerota, W., Pilkey, J., Ngin, T., Moore, R., Rassou, H., Cummer, S., Grove, J., Nag, A., Betten, D., and Bozarth, A.: Ground-level observation of a terrestrial gamma ray flash initiated by a triggered lightning, J. Geophys. Res.-Atmos., 121, 6511–6533, https://doi.org/10.1002/2015JD024426, 2016.

Hazelton, B. J., Grefenstette, B. W., Smith, D. M., Dwyer, J. R., Shao, X.-M., Cummer, S. A., Chronis, T., Lay, E. H., and Holzworth, R. H.: Spectral dependence of terrestrial gamma-ray flashes on source distance, Geophys. Res. Lett., 36, L01108, https://doi.org/10.1029/2008GL035906, 2009.

Helmerich, C., McKinney, T., Cavanaugh, E., and Dangelo, S.: TGFs, gamma-ray glows, and direct lightning strike radiation observed during a single flight of a balloon-borne gamma-ray spectrometer, Earth Space Sci., 11, e2023EA003317, https://doi.org/10.1029/2023EA003317, 2024.

Kochkin, P., Sarria, D., Lehtinen, N., Mezentsev, A., Yang, S., Genov, G., Ullaland, K., Marisaldi, M., Østgaard, N., Christian, H. J., Grove, J., Quick, M., Al-Nussirat, S., and Wulf, E.: A rapid gamma-ray glow flux reduction observed from 20 km altitude, J. Geophys. Res.-Atmos., 126, e2020JD033467, https://doi.org/10.1029/2020JD033467, 2021.

Kolmašová, I., Santolík, O., Šlegl, J., Popová, J., Sokol, Z., Zacharov, P., Ploc, O., Diendorfer, G., Langer, R., Lán, R., and Strhárský, I.: Continental thunderstorm ground enhancement observed at an exceptionally low altitude, Atmos. Chem. Phys., 22, 7959–7973, https://doi.org/10.5194/acp-22-7959-2022, 2022.

Lindanger, A., Marisaldi, M., Sarria, D., Østgaard, N., Lehtinen, N., Skeie, C., Mezentzev, A., Kochkin, P., Ullaland, K., Yang, S., Genov, G., Carlson, B., Köhn, C., Navarro-Gonzalez, J., Connell, P., Reglero, V., and Neubert, T.: Spectral analysis of individual terrestrial gamma-ray flashes detected by ASIM, J. Geophys. Res.-Atmos., 126, e2021JD035347, https://doi.org/10.1029/2021JD035347, 2021.

Lyu, F., Zhang, Y., Lu, G., Zhu, B., Zhang, H., Xu, W., Xiong, S., and Lyu, W.: Recent observations and research progresses of terrestrial gamma-ray flashes during thunderstorms, Science China Earth Sciences, 66, 435–455, https://doi.org/10.1007/s11430-022-1026-y, 2023.

Maia, J., da Silva, R. C., and Mingacho, J.: Evaluation of effective dose for gamma-rays of terrestrial gamma-ray flashes in aviation: spectral-and atmosphere-effects, Radiat. Phys. Chem., 215, 111332, https://doi.org/10.1016/j.radphyschem.2023.111332, 2024.

Mailyan, B., Briggs, M., Cramer, E., Fitzpatrick, G., Roberts, O., Stanbro, M., Connaughton, V., McBreen, S., Bhat, P., and Dwyer, J.: The spectroscopy of individual terrestrial gamma-ray flashes: Constraining the source properties, J. Geophys. Res.-Space, 121, 11–346, https://doi.org/10.1002/2016JA022702, 2016.

Mailyan, B., Xu, W., Celestin, S., Briggs, M., Dwyer, J., Cramer, E., Roberts, O., and Stanbro, M.: Analysis of individual terrestrial gamma-ray flashes with lightning leader models and fermi gamma-ray burst monitor data, J. Geophys. Res.-Space, 124, 7170–7183, https://doi.org/10.1029/2019JA026912, 2019.

Maiorana, C., Marisaldi, M., Lindanger, A., Østgaard, N., Ursi, A., Sarria, D., Galli, M., Labanti, C., Tavani, M., Pittori, C., and Verrecchia, F.: The 3rd AGILE terrestrial gamma-ray flashes catalog. Part II: Optimized selection criteria and characteristics of the new sample, J. Geophys. Res.-Atmos., 125, e2019JD031986, https://doi.org/10.1029/2019JD031986, 2020.

Maiorana, C., Marisaldi, M., Füllekrug, M., Soula, S., Lapierre, J., Mezentsev, A., Skeie, C., Heumesser, M., Chanrion, O., Østgaard, N., Neubert, T., and Reglero, V.: Observation of terrestrial gamma-ray flashes at mid latitude, J. Geophys. Res.-Atmos., 126, e2020JD034432, https://doi.org/10.1029/2020JD034432, 2021.

Marisaldi, M., Fuschino, F., Labanti, C., Galli, M., Longo, F., Del Monte, E., Barbiellini, G., Tavani, M., Giuliani, A., Moretti, E., Vercellone, S., Costa, E., Cutini, S., Donnarumma, I., Evangelista, Y., Feroci, M., Lapshov, I., Lazzarotto, F., Lipari, P., Mereghetti, S., Pacciani, L., Rapisarda, M., Soffitta, P., Trifoglio, M., Argan, A., Boffelli, F., Bulgarelli, A., Caraveo, P., Cattaneo, P., Chen, A., Cocco, V., D'Ammando, F., De Paris, G., Di Cocco, G., Di Persio, G., Ferrari, A., Fiorini, M., Froysland, T., Gianotti, F., Morselli, A., Pellizzoni, A., Perotti, F., Picozza, P., Piano, G., Pilia, M., Prest, M., Pucella, G., Rappoldi, A., Rubini, A., Sabatini, S., Striani, E., Trois, A., Vallazza, E., Vittorini, V., Zambra, A., Zanello, D., Antonelli, L., Colafrancesco, S., Gasparrini, D., Giommi, P., Pittori, C., Preger, B., Santolamazza, P., Verrecchia, F., and Salotti, L.: Detection of terrestrial gamma ray flashes up to 40 MeV by the AGILE satellite, J. Geophys. Res.-Space, 115, A00E13, https://doi.org/10.1029/2009JA014502, 2010.

Marisaldi, M., Fuschino, F., Tavani, M., Dietrich, S., Price, C., Galli, M., Pittori, C., Verrecchia, F., Mereghetti, S., Cattaneo, P., Colafrancesco, S., Argan, A., Labanti, C., Longo, F., Del Monte, E., Barbiellini, G., Giuliani, A., Bulgarelli, A., Campana, R., Chen, A., Gianotti, F., Giommi, P., Lazzarotto, F., Morselli, A., Rapisarda, M., Rappoldi, A., Trifoglio, M., Trois, A., and Vercellone, S.: Properties of terrestrial gamma ray flashes detected by AGILE MCAL below 30 MeV, J. Geophys. Res.-Space, 119, 1337–1355, https://doi.org/10.1002/2013JA019301, 2014.

Marisaldi, M., Galli, M., Labanti, C., Østgaard, N., Sarria, D., Cummer, S., Lyu, F., Lindanger, A., Campana, R., Ursi, A., Tavani, M., Fuschino, F., Argan, A., Trois, A., Pittori, C., and Verrecchia, F.: On the high-energy spectral component and fine time structure of terrestrial gamma ray flashes, J. Geophys. Res.-Atmos., 124, 7484–7497, https://doi.org/10.1029/2019JD030554, 2019.

Marisaldi, M., Østgaard, N., Mezentsev, A., Lang, T., Grove, J. E., Shy, D., Heymsfield, G. M., Krehbiel, P., Thomas, R., Stanley, M., Sarria, D., Schultz, C., Blakeslee, R., Quick, M., Christian, H., Adams, I., Kroodsma, R., Lehtinen, N., Ullaland, K., Yang, S., Hasan Qureshi, B., Søndergaard, J., Husa, B., Walker, D., Bateman, M., Mach, D., Cummer, S., Pazos, M., Pu, Y., Bitzer, P., Fullekrug, M., Cohen, M., Montanya, J., Younes, C., van der Velde, O., Roncancio, J., Lopez, J., Urbani, M., and Santos, A.: Highly dynamic gamma-ray emissions are common in tropical thunderclouds, Nature, 634, 57–60, https://doi.org/10.1038/s41586-024-07936-6, 2024.

Neubert, T., Østgaard, N., Reglero, V., Blanc, E., Chanrion, O., Oxborrow, C. A., Orr, A., Tacconi, M., Hartnack, O., and Bhanderi, D. D.: The ASIM mission on the international space station, Space Sci. Rev., 215, 1–17, https://doi.org/10.1007/s11214-019-0592-z, 2019.

Østgaard, N., Gjesteland, T., Hansen, R., Collier, A., and Carlson, B.: The true fluence distribution of terrestrial gamma flashes at satellite altitude, J. Geophys. Res.-Space, 117, A03327, https://doi.org/10.1029/2011JA017365, 2012.

Østgaard, N., Neubert, T., Reglero, V., Ullaland, K., Yang, S., Genov, G., Marisaldi, M., Mezentsev, A., Kochkin, P., Lehtinen, N., Sarria, D., Hasan Qureshi, S., Solberg, A., Maiorana, C., Albrechtsen, K., Budtz-Jørgensen, C., Kuvvetli, I., Christiansen, F., Chanrion, O., Heumesser, M., Navarro-Gonzalez, J., P, C., Eyles, C., Christian, H., and Al-nussirat, S.: First 10 months of TGF observations by ASIM, J. Geophys. Res.-Atmos., 124, 14024–14036, https://doi.org/10.1029/2019JD031214, 2019.

Østgaard, N., Cummer, S. A., Mezentsev, A., Luque, A., Dwyer, J., Neubert, T., Reglero, V., Marisaldi, M., Kochkin, P., Sarria, D., Lehtinen, N., Ullaland, K., Yang, S., Genov, G., Chanrion, O., Christiansen, F., and Pu, Y.: Simultaneous observations of EIP, TGF, Elve, and optical lightning, J. Geophys. Res.-Atmos., 126, e2020JD033921, https://doi.org/10.1029/2020JD033921, 2021.

Ostgaard, N., Lang, T., Marisaldi, M., Grove, E., Quick, M., Christian, H., Schultz, C., Blakeslee, R., Adams, I., Kroodsma, R., Heymsfield, G., Mezentsev, A., Sarria, D., Bjorg Engeland, I., Fuglestad, A., Lehtinen, N., Ullaland, K., Yang, S., Hasan Qureshi, B., and Sondergaard, J. and the ALOFT team: TGF and gamma-ray glow highlights from the ALOFT 2023 flight campaign, EGU General Assembly 2024, Vienna, Austria, 14–19 Apr 2024, EGU24-7900, https://doi.org/10.5194/egusphere-egu24-7900, 2024a.

Østgaard, N., Mezentsev, A., Marisaldi, M., Grove, J., Quick, M., Christian, H., Cummer, S., Pazos, M., Pu, Y., Stanley, M., Sarria, D., Lang, T., Schultz, C., Blakeslee, R., Adams, I., Kroodsma, R., Heymsfield, G., Lehtinen, N., Ullaland, K., Yang, S., Hasan Qureshi, B., Søndergaard, J., Husa, B., Walker, D., Shy, D., Bateman, M., Bitzer, P., Fullekrug, M., Cohen, M., Montanya, J., Younes, C., van der Velde, O., Krehbiel, P., Roncancio, J., Lopez, J., Urbani, M., Santos, A., and Mach, D.: Flickering gamma-ray flashes, the missing link between gamma glows and TGFs, Nature, 634, 53–56, https://doi.org/10.1038/s41586-024-07893-0, 2024b.

Pallu, M., Celestin, S., Trompier, F., and Klerlein, M.: Estimation of radiation doses delivered by terrestrial gamma ray flashes within leader-based production models, J. Geophys. Res.-Atmos., 126, e2020JD033907, https://doi.org/10.1029/2020JD033907, 2021.

Pallu, M., Celestin, S., Hazem, Y., Trompier, F., and Patton, G.: XStorm: A new gamma ray spectrometer for detection of close proximity gamma ray glows and TGFs, J. Geophys. Res.-Atmos., 128, e2023JD039180, https://doi.org/10.1029/2023JD039180, 2023.

Petrov, N.: Synchrotron mechanism of X-ray and gamma-ray emissions in lightning and spark discharges, Sci. Rep., 11, 19824, https://doi.org/10.1038/s41598-021-99336-3, 2021.

Picone, J., Hedin, A., Drob, D. P., and Aikin, A.: NRLMSISE-00 empirical model of the atmosphere: Statistical comparisons and scientific issues, J. Geophys. Res.-Space, 107, SIA–15, https://doi.org/10.1029/2002JA009430, 2002.

Popová, J., Sokol, Z., Wang, P., and Svoboda, J.: Observations and modelling of the winter thunderstorm on 4 February 2022 at the Milešovka meteorological observatory, Q. J. Roy. Meteor. Soc., 149, 3541–3561, https://doi.org/10.1002/qj.4572, 2023.

Roberts, O., Fitzpatrick, G., Stanbro, M., McBreen, S., Briggs, M., Holzworth, R., Grove, J., Chekhtman, A., Cramer, E., and Mailyan, B.: The first Fermi-GBM terrestrial gamma ray flash catalog, J. Geophys. Res.-Space, 123, 4381–4401, https://doi.org/10.1029/2017JA024837, 2018.

Rutjes, C., Sarria, D., Skeltved, A. B., Luque, A., Diniz, G., Østgaard, N., and Ebert, U.: Evaluation of Monte Carlo tools for high energy atmospheric physics, Geosci. Model Dev., 9, 3961–3974, https://doi.org/10.5194/gmd-9-3961-2016, 2016.

Rutjes, C., Diniz, G., Ferreira, I., and Ebert, U.: TGF afterglows: A new radiation mechanism from thunderstorms, Geophys. Res. Lett., 44, 10–702, https://doi.org/10.1002/2017GL075552, 2017.

Sarria, D., Rutjes, C., Diniz, G., Luque, A., Ihaddadene, K. M. A., Dwyer, J. R., Østgaard, N., Skeltved, A. B., Ferreira, I. S., and Ebert, U.: Evaluation of Monte Carlo tools for high-energy atmospheric physics II: relativistic runaway electron avalanches, Geosci. Model Dev., 11, 4515–4535, https://doi.org/10.5194/gmd-11-4515-2018, 2018.

Skeltved, A. B., Østgaard, N., Carlson, B., Gjesteland, T., and Celestin, S.: Modeling the relativistic runaway electron avalanche and the feedback mechanism with GEANT4, J. Geophys. Res.-Space, 119, 9174–9191, https://doi.org/10.1002/2014JA020504, 2014.

Sommer, M.: Mesh data + tally data, figshare [data set], https://doi.org/10.6084/m9.figshare.28612058.v1, 2025.

Smith, D., Dwyer, J., Hazelton, B., Grefenstette, B., Martinez-McKinney, G., Zhang, Z., Lowell, A., Kelley, N., Splitt, M., Lazarus, S., Ulrich, W., Schaal, M., Saleh, Z., Cramer, E., Rassoul, H., Cummer, S., Lu, G., Shao, X., Ho, C., Hamlin, T., Blakeslee, R., and Heckman, S.: A terrestrial gamma ray flash observed from an aircraft, J. Geophys. Res.-Atmos., 116, D20124, https://doi.org/10.1029/2011JD016252, 2011.

Smith, D. M., Lopez, L. I., Lin, R. P., and Barrington-Leigh, C. P.: Terrestrial gamma-ray flashes observed up to 20 MeV, Science, 307, 1085–1088, https://doi.org/10.1126/science.1107466, 2005.

Stadnichuk, E., Svechnikova, E., Nozik, A., Zemlianskaya, D., Khamitov, T., Zelenyy, M., and Dolgonosov, M.: Relativistic runaway electron avalanches within complex thunderstorm electric field structures, J. Geophys. Rese.-Atmos., 126, e2021JD035278, https://doi.org/10.1029/2021JD035278, 2021.

Stadnichuk, E., Zemlianskaya, D., Svechnikova, E., Kim, E., Sedelnikov, A., and Anuaruly, O.: Simple reactor model of relativistic runaway electron avalanche development, arXiv [preprint], https://doi.org/10.48550/arXiv.2301.00542, 2023.

Stránský, V., Istokskaia, V., Versaci, R., Giuffrida, L., Cimmino, A., Margarone, D., and Olšovcová, V.: Development, optimization, and calibration of an active electromagnetic calorimeter for pulsed radiation spectrometry, J. Instrum., 16, P08060, https://doi.org/10.1088/1748-0221/16/08/P08060, 2021.

Tavani, M., Marisaldi, M., Labanti, C., Fuschino, F., Argan, A., Trois, A., Giommi, P., Colafrancesco, S., Pittori, C., Palma, F., Trifoglio, M., Gianotti, F., Bulgarelli, A., Vittorini, A., Verrecchia, F., Salotti, L., Barbiellini, G., Caraveo, P., Cattaneo, P., Chen, A., Contessi, T., Costa, E., D'Ammando, F., Del Monte, E., De Paris, G., Di Cocco, G., Di Persio, G., Donnarumma, I., Evangelista, Y., Feroci, M., Ferrari, A., Galli, M., Giuliani, A., Giusti, M., Lapshov, I., Lazzarotto, F., Lipari, P., Longo, F., Mereghetti, S., Morelli, E., Moretti, E., Morselli, A., Pacciani, L., Pellizzoni, A., Perotti, F., Piano, G., Picozza, P., Pilia, M., Pucella, G., Prest, M., Rapisarda, M., Rappoldi, A., Rossi, E., Rubini, A., Sabatini, S., Scalise, E., Soffitta, P., Striani, E., Vallazza, E., Vercellone, S., Zambra, A., and Zanello, D.: Terrestrial gamma-ray flashes as powerful particle accelerators, Phys. Rev. Lett., 106, 018501, https://doi.org/10.1103/PhysRevLett.106.018501, 2011.

Tavani, M., Argan, A., Paccagnella, A., Pesoli, A., Palma, F., Gerardin, S., Bagatin, M., Trois, A., Picozza, P., Benvenuti, P., Flamini, E., Marisaldi, M., Pittori, C., and Giommi, P.: Possible effects on avionics induced by terrestrial gamma-ray flashes, Nat. Hazards Earth Syst. Sci., 13, 1127–1133, https://doi.org/10.5194/nhess-13-1127-2013, 2013.

Tran, M., Rakov, V., Mallick, S., Dwyer, J., Nag, A., and Heckman, S.: A terrestrial gamma-ray flash recorded at the Lightning Observatory in Gainesville, Florida, J. Atmos. Sol.-Terr. Phy., 136, 86–93, https://doi.org/10.1016/j.jastp.2015.10.010, 2015.

Ursi, A., Rodriguez Fernandez, G., Tiberia, A., Virgilli, E., Arnone, E., Preziosi, E., Campana, R., and Tavani, M.: A study on tgf detectability at 2165 m altitude: Estimates for the mountain-based gamma-flash experiment, Remote Sens., 14, 3103, https://doi.org/10.3390/rs14133103, 2022.

Wada, Y., Enoto, T., Nakazawa, K., Furuta, Y., Yuasa, T., Nakamura, Y., Morimoto, T., Matsumoto, T., Makishima, K., and Tsuchiya, H.: Downward terrestrial gamma-ray flash observed in a winter thunderstorm, Phys. Rev. Lett., 123, 061103, https://doi.org/10.1103/PhysRevLett.123.061103, 2019.

Wada, Y., Enoto, T., Nakazawa, K., Odaka, H., Furuta, Y., and Tsuchiya, H.: Photonuclear reactions in lightning: 1. Verification and modeling of reaction and propagation processes, J. Geophys. Res.-Atmos., 125, e2020JD033193, https://doi.org/10.1029/2020JD033193, 2020.

Wallace, J. M. and Hobbs, P. V.: Atmospheric science: an introductory survey, vol. 92, Elsevier, ISBN 0080499538, 9780080499536, 2006.

Zelenyi, M., Nozik, A., and Stadnichuk, E.: Reactor like TGE model, in: AIP Conference Proceedings, vol. 2163, 060005–1-060005, AIP Publishing, https://doi.org/10.1063/1.5130111, 2019.